WELDING RESEARCH

SUPPLEMENT TO THE WELDING JOURNAL, MAY, 1985

Sponsored by the American Welding Society and the Welding Research Council

TECHNICAL PAPERS EDITOR: T.P. SCHOONMAKER

Readers are advised that all papers published in the *Welding Journal's* Research Supplement undergo Peer Review before publication for: 1) originality of the contribution; 2) technical value to the welding community; 3) prior publication of the material being reviewed; 4) proper credit to others working in the same area; and 5) justification of the conclusions based on the results.

The names of the more than 160 individuals serving on the AWS Peer Review Panel are published periodically. All are experts in their respective technical areas, and all are volunteers in the program.

Hot-Cracking Studies of Alloy CN-7M

Testing indicates that S, P, and Si are responsible for the hot cracking tendency of CN-7M

BY M. J. CIESLAK AND W. F. SAVAGE

ABSTRACT. An investigation was performed to determine the causes of hot-cracking in cast alloy CN-7M. Differential thermal analysis results indicated that CN-7M does not have an extremely wide solidification temperature range. Varestraint hot-cracking tests were performed on two sets of factorial-designed alloys. Results of these tests indicate that sulfur, phosphorus, and silicon are responsible for the hot-cracking tendency of alloy CN-7M.

The mechanism of cracking was found to be related to the segregation of impurity elements to solidification grain boundaries. Silicon additions caused a thin film M_6C carbide/austenite eutectic to form which severely reduced the resistance to hot-cracking of alloy CN-7M. Solidification quench experiments were performed to determine the segregation pattern of solute elements during solidification. All elements analyzed (Ni, Cr, Cu, Mo, Mn, Si, S, P) were found to segregate to interdendritic volumes during solidification.

Introduction

CN-7M* is a wholly austenitic stainless steel casting alloy designed for use in a variety of aqueous environments, especially sulfuric acid. The composition of alloy CN-7M (27.5-30.5% Ni, 19-22% Cr, 3-4% Cu, 2-3% Mo, 1.5% max. Mn, 1.5% max. Si, 0.07% max. C, 0.04% max. S, 0.04% max. P, bal. Fe) places it in the class of alloys known as the super-stainless steels.

From the standpoint of welding and casting, alloy CN-7M possesses the susceptibility to hot-cracking found in other wholly austenitic stainless steels and nickel-base alloys. Unlike many 300-series stainless steels, the composition limits of alloy CN-7M are such that a primary delta-ferrite solidification mode cannot occur. The reduction in hot-cracking susceptibility accompanying a primary delta-ferrite solidification mode is, therefore, not possible in this alloy system.

The objectives of this project were to determine the compositional variables which influence fusion-zone hot-cracking in weldments of alloys CN-7M and to establish the hot-cracking mechanism.

*CN-7M is a Steel Founders Society of America (ACI) designation; the equivalent SAE/ASTM unified number is J95150.

Paper presented at the 65th Annual AWS Convention held in Dallas, Texas, during April 8-13, 1984.

M. J. CIESLAK is with Sandia National Laboratories, Albuquerque, New Mexico, and W. F. SAVAGE is Professor Emeritus, Rensselaer Polytechnic Institute, Troy, New York.

Materials and Procedures

The alloys used in this study were supplied by the Steel Founders Society of America. The compositions of these alloys are given in Table 1, and were determined by wet chemical analysis (except for carbon and sulfur, which were analyzed using the combustion technique). The compositions shown for heats 1-16 and 31 represent the average of three analyses. Those for heats 17-30 are the average of two analyses. Heats 1-16 comprise a ¼-fractional factorial design of alloys chosen from a complete six-factor, two-level design. In this series, the six factors are nickel, copper, molybdenum, silicon, chromium, and manganese. All other elements are held essentially constant, except iron, the level of which is dependent on the level of the six variable factors. Figure 1 shows, in matrix form, the balanced nature of this design. Both levels of each factor are contained exactly eight times.

Heats 17-30 were used during a full factorial study of the effects of carbon, silicon, sulfur, and phosphorus on hot-cracking susceptibility. The remainder of the alloying elements were held at levels roughly in the center of the alloy composition range. A full factorial, two-level set of alloys containing four factors would require the melting of 16 heats. During the processing of the 16 heats, a required

Table 1—Alloy Compositions[a]

Heat No.	Ni	Cu	Mn	Mo	5i	Cr	C	P	5
1	28.55	2.58	0.13	2.06	0.14	17.93	0.021	0.011	0.010
2	33.27	2.64	0.12	2.07	1.31	20.93	0.020	0.011	0.008
3	27.89	3.90	0.11	2.04	0.29	20.99	0.019	0.011	0.008
4	33.17	4.15	0.11	2.05	1.30	18.40	0.034	0.011	0.007
5	27.95	2.59	1.27	2.11	1.24	22.51	0.018	0.013	0.007
6	32.69	2.63	1.19	2.03	0.26	19.00	0.017	0.007	0.008
7	27.90	3.94	1.32	2.01	1.18	18.75	0.017	0.010	0.007
8	33.10	4.06	1.29	1.98	0.22	20.95	0.016	0.010	0.008
9	27.67	2.56	0.14	3.48	1.30	18.24	0.018	0.010	0.008
10	33.13	2.69	0.21	3.46	0.17	21.86	0.017	0.011	0.009
11	28.08	3.98	0.20	3.53	1.18	22.04	0.016	0.010	0.009
12	33.14	4.04	0.18	3.44	0.21	19.03	0.016	0.010	0.009
13	27.94	2.64	1.13	3.52	0.27	21.45	0.014	0.011	0.008
14	33.01	2.66	1.15	3.44	1.13	18.22	0.015	0.011	0.009
15	28.06	3.97	1.12	3.48	0.25	18.07	0.015	0.010	0.008
16	33.31	4.18	1.35	3.56	1.18	22.00	0.019	0.013	0.008
17	28.91	3.47	0.53	2.74	0.14	20.09	0.017	0.007	0.004
18	28.61	3.46	0.53	2.79	0.14	19.63	0.066	0.005	0.005
19	29.02	3.57	0.52	2.75	0.93	20.12	0.019	0.008	0.006
20	29.02	3.55	0.57	2.77	0.92	19.84	0.066	0.008	0.005
21	28.82	3.39	0.43	2.78	0.15	19.85	0.015	0.007	0.022
22	28.49	3.42	0.56	2.72	0.15	19.91	0.053	0.008	0.015
23	28.94	3.53	0.53	2.77	0.97	20.05	0.018	0.008	0.017
24	28.72	3.48	0.53	2.76	1.00	19.85	0.047	0.008	0.018
25	28.86	3.48	0.52	2.71	0.16	20.02	0.010	0.020	0.004
26	28.91	3.46	0.53	2.70	0.19	19.93	0.048	0.023	0.003
27	29.00	3.53	0.52	2.75	1.02	20.00	0.012	0.021	0.005
28	29.02	3.57	0.52	2.77	0.90	20.09	0.044	0.020	0.005
29	28.83	3.52	0.52	2.73	0.19	19.95	0.009	0.022	0.020
30	28.99	3.52	0.51	2.72	0.90	20.00	0.012	0.022	0.018
31	34.15	3.96	1.31	3.37	1.40	21.25	0.130	0.010	0.007

[a]All compositions in weight-percent, balance iron.

carbon addition was left out of two heats. Because of this, only 14 heats were available for testing. It was felt that it would be inappropriate to melt two heats separately at a later date to fill in for the two losses because conditions and raw materials could not be reproduced exactly. During the subsequent data analysis, a missing value routine was used to estimate the unavailable data from these heats.

All alloys used in this study were produced by the split-heat technique, and all were made from high purity virgin components. They were vacuum-induction melted and investment cast to near-net shape as rectangular bars approximately 6½ in. (165 mm) long, 2 in. (51 mm) wide, and ½ in. (12.7 mm) thick. No deoxidizing agent was added to the melts and no heat treatment was performed on the alloys subsequent to casting. The castings were all finish machined to a thickness of 0.450 ± 0.010 in. (11.4 ± 0.25 mm) prior to testing.

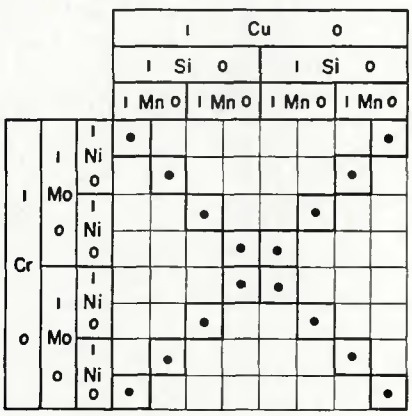

Fig. 1—Matrix form for factorial design used during investigation

Hot-cracking susceptibility was quantified with the Varestraint Test (Refs. 1,2). All specimens were tested at 1.8% augmented strain and replicated three times. This provided an internal measure of experimental variance.

All welding was done using autogenous, straight-polarity, gas-tungsten-arc (GTA) welding. Welding conditions were 260 A, 12.5 V, and 4 ipm (1.69 mm/s) travel speed under a 40 cfh (18.9 L/min) argon shielding gas. A single cylinder of ultra-high purity argon (99.998% Ar) was used as a source of shielding gas for all welds. The order of testing for each run of samples was determined from a random numbers table. The Total Crack Length was used as the index of cracking tendency. This number is the summation of the length of all fusion zone cracks found on the as-welded surface propagating back from the location of the solid-liquid interface at the instant of straining.

Elemental segregation during solidification was investigated with a water quench technique similar to that described by Arata *et al.* (Ref 3). When a steady-state bead-on-plate weld was established, a high-pressure, water-spray quench simultaneously decanted the weld pool and rapidly quenched the weld metal, which was in the process of solidifying along the trailing edge of the weld. The tips of the dendrites, which were growing into the liquid at the instant of quenching, were revealed by optical microscopy. These dendrites and their associated interdendritic volumes were analyzed with an electron microprobe, revealing the pattern of segregation accompanying solidification.

Differential thermal analysis (DTA) was performed on selected heats of material with a Mettler Thermoanalyzer. Specimens from the castings were heated under a helium atmosphere in an alumina crucible to approximately 50°C (90°F) above the liquidus, and then cooled at a constant rate of 6°C/min (10.8°F/min) through the solidification temperature range. Liquidus and solidus temperatures and the solidification temperature range were thus determined for the selected alloys.

Table 2—Factorial Design Levels, wt-%

Factor	Low level	St. dev.[a]	High level	St. dev.[a]
		Major element factorial design		
Ni	28.00	0.55	33.10	0.34
Cu	2.62	0.06	4.03	0.13
Mn	0.15	0.06	1.23	0.10
Mo	2.04	0.06	3.49	0.13
Si	0.23	0.06	1.23	0.07
Cr	18.43	0.47	21.59	0.63
		Minor element factorial design		
C	0.014	0.004	0.054	0.009
P	0.007	0.001	0.021	0.001
S	0.005	0.001	0.018	0.002
Si	0.16	0.02	0.95	0.05

[a]St. dev = standard deviation.

Electron probe microanalysis was conducted using both a JEOL Superprobe and a Cameca microprobe. A JEOL JSEM-200 TEM/STEM was used in the analysis of minor phases. This microscope is equipped with a Nuclear Semiconductor energy dispersive x-ray detector and a Tracor Northern NS 880 analyzer for elemental data acquisition. Both extraction replicas and thin foils of welds and the associated hot-cracks were examined.

Experimental Design and Analysis

From a compositional standpoint, hot-cracking can occur in an alloy because of three reasons:

1. The nominal alloy composition, excluding impurities, is such that the material has a wide solidification temperature range.

2. An intentional alloy addition causes the formation of a low melting point constituent, such as a eutectic, which could wet solidification grain boundaries at temperatures well below the equilibrium solidus.

3. This reason is related to alloy cleanliness, *i.e.*, certain elemental impurities strongly segregate to interdendritic regions and solidification grain boundaries where they either form unwanted, low melting point, non-equilibrium constituents, or they lower the surface tension of the final solidifying liquid; either condition is harmful from a hot-cracking standpoint.

This study is designed to investigate all three of the above cases. The initial investigation is concerned with identifying the effects, if any, of the major alloying elements on hot-cracking. The elements nickel, chromium, copper, molybdenum, manganese, and silicon are intentional alloying additions to CN-7M.

A factorial design was constructed of these six elements at two levels, roughly corresponding to the extremes of the compositional range for each component. A six-factor, two-level design requires 64 different combinations. Since that number of alloys, all made from the same batch of raw materials, was impractical, a fractional-factorial design was employed, in which 16 heats were required. The design, shown in matrix form in Fig. 1, was chosen (Refs. 4,5) such that single element effects are confounded only with third-order and higher interactions. The advantage of a factorial-type design is that when analysis is complete, the conclusions are not tied to one specific chemistry, but are general in nature for the range of compositions studied.

Subsequent to investigating the major element effects, the effects of the minor elements, carbon, sulfur, and phosphorus, were studied by means of a full-factorial examination. In addition, silicon was added as a fourth factor because of the magnitude of its effect as determined in the initial design. The levels of the factors in this series were chosen as those one would expect from normal melt practice (high level) and those which represent state-of-the-art melting capabilities (low level).

Table 2 gives the average values and standard deviations of the high and low levels of the factors used in each of the factorial designs.

The method of Yates (Ref. 6) was used in the statistical analysis of the Varestraint data. This is a systematic procedure to reduce raw factorial test data to factor effects using an analysis of variance.

Results

Varestraint Testing

Table 3 gives the results of Varestraint testing of all alloys. It should be noted that the sum of all data in any one run from a given design differs by less than 4% from the sum of data in either of the other two runs from that same design.

Table 3—Varestraint Test Total Crack Length Data[a]

Heat no.	Run 1	Run 2	Run 3	Average
		Major element factorial		
1	0.333	0.372	0.304	0.336
2	0.419	0.661	0.670	0.583
3	0.350	0.214	0.221	0.262
4	0.503	0.585	0.610	0.566
5	0.592	0.446	0.638	0.559
6	0.260	0.357	0.259	0.292
7	0.664	0.517	0.701	0.627
8	0.199	0.187	0.296	0.227
9	0.647	0.410	0.439	0.499
10	0.252	0.163	0.126	0.180
11	0.598	0.406	0.482	0.495
12	0.253	0.171	0.222	0.215
13	0.085	0.274	0.200	0.186
14	0.513	0.666	0.481	0.553
15	0.204	0.356	0.190	0.250
16	0.693	0.555	0.482	0.577
Sum	6.565	6.340	6.321	—
		Minor element factorial design		
17	0.053	0.034	0.063	0.050
18	0.014	0.029	0.012	0.018
19	0.253	0.363	0.242	0.286
20	0.099	0.110	0.141	0.117
21	0.402	0.281	0.297	0.327
22	0.355	0.368	0.344	0.356
23	0.584	0.563	0.464	0.537
24	0.389	0.350	0.486	0.408
25	0.304	0.277	0.252	0.278
26	0.252	0.293	0.278	0.274
27	0.441	0.401	0.462	0.435
28	0.299	0.475	0.380	0.385
29	0.576	0.370	0.464	0.470
30	0.606	0.744	0.626	0.659
Sum	4.627	4.658	4.511	—

[a]All values in inches.

The results of the Yates analysis from the two sets of alloys are shown in graphical form in Figs. 2 and 3. The horizontal dotted line on the two graphs represents the 90% significance level for effects measured in the given design. This level is essentially the value below which an effect cannot be distinguished from the experimental variance.

Among the major alloying elements, only silicon has a statistically significant effect and that effect is highly detrimental (positive values of an effect imply an increase in total crack length). This analysis implies that compositional variations among the major alloying elements, with the exception of silicon, will have no effect on hot-cracking properties.

Among the minor elements, sulfur, phosphorus, and silicon all have detrimental effects on hot-cracking, while carbon by itself has essentially no effect. There are interactive effects between carbon and the other factors. Carbon tends to increase the detrimental effects of both sulfur and phosphorus, while it diminishes the detrimental effect of silicon.

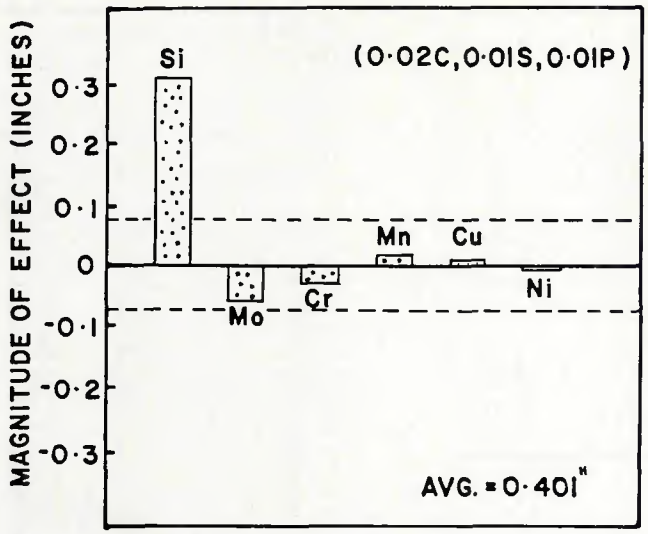

Fig. 2—Results of Yates analysis for heats 1-16

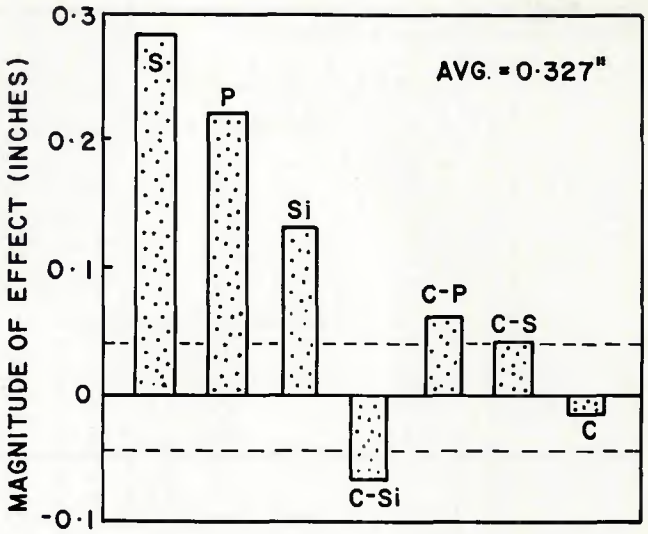

Fig. 3—Results of Yates analysis for heats 17-30

Differential Thermal Analysis

Heats 1, 4, 14, and 16 were studied by differential thermal analysis, as described earlier. Table 4 lists the liquidus, solidus, and solidification temperature range for the four heats of CN-7M tested. Other investigators have reported (Ref. 25) a reproducibility of solidus and liquidus temperatures of ±2°C (3.6°F) when using the same equipment to study the solidification behavior of other austenitic stainless steels. Table 4 also gives the same data for other stainless steels including wholly austenitic grades (Types 310 and 904-L), duplex austenitic-ferritic alloys (CF-8M as well as Types 308, 304, and 304-L), and ferritic stainless steels.

The cooling rates used were not the same for all alloys. However, a general trend can be seen which indicates that, for a given alloy, the solidification range increases with increasing cooling rate.

There was no indication of the formation of a second phase, or constituent, from the liquid during the differential thermal analyses. It is important to understand, though, that it is extremely difficult to detect reactions involving less than 1% of the bulk material. This implies that the potential formation of thin film eutectics could go undetected.

Table 4—Differential Thermal Analysis Results

Heat No.	Cooling rate, °C/min	Liquidus, °C	Solidus, °C	Solidification temperature range, °C
1	6	1399	1337	62
4	6	1335	1268	67
14	6	1326	1252	74
16	6	1340	1241	99
Alloy type:				
CF-8M (Ref. 24)	4	1423	1355	68
CF-8M (Ref. 24)	4	1421	1349	72
308 (Ref. 25)	6	1435	1355	80
310 (Ref. 25)	6	1395	1304	91
308 (Ref. 26)	20	1435	1339	96
304 (Ref. 27)	5	1456	1399	57
	15	1457	1395	62
	35	1456	1371	85
304-L (Ref. 27)	5	1462	1420	42
	15	1462	1401	61
	35	1463	1398	65
904-L (Ref. 27)	5	1397	1332	65
	15	1397	1315	82
	35	1396	1300	96
Fe-25CR-22Ni-2Mo (Ref. 28)	2	1401	1335	66
310 (Ref. 28)	2	1399	1315	80
Fe-19Cr-25Ni-4Mo −1.5Cu (Ref. 28)	2	1389	1305	84
800 (Ref. 28)	2	1399	1280	119
Fe-18Cr-2Mo-Ti (Ref. 29)	6	1496	1440	56
Fe-25Cr-4Ni-4Mo −Ti (Ref. 29)	6	1470	1395	75

Microscopy

Optical metallography performed on the Varestraint specimens revealed the hot-cracks to be intergranular in nature. Figure 4 shows a hot-crack extending from the fusion zone back into the heat-affected-zone along a prior casting grain boundary. Higher magnification images of the fusion zone hot-cracks indicated the presence of a minor constituent along the solidification grain boundaries only in those alloys containing the high level of silicon. An example of this is shown in Fig. 5.

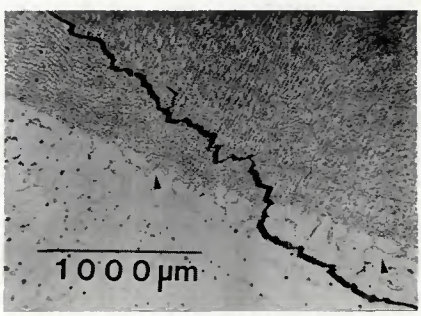

Fig. 4—Hot crack extending along a prior casting grain boundary, Heat 7. Arrow denotes regions of partial melting in the as-cast base metal

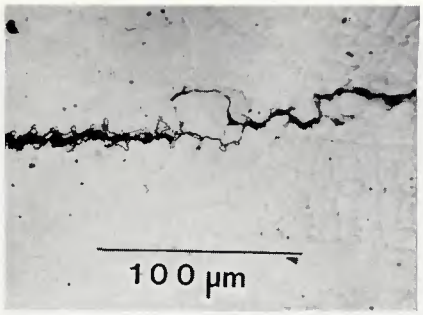

Fig. 5—Fusion zone hot-crack along a eutectic M_6C-coated solidification grain boundary, Heat 16

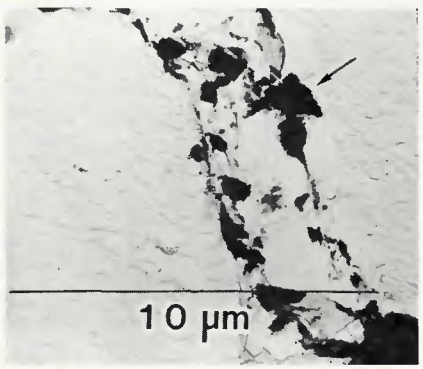

Fig. 6—Extraction replica of eutectic M_6C Carbide (arrow) along fusion zone hot crack, Heat 16

Fig. 7—Diffraction pattern of phase denoted by arrow in Fig. 6

In an attempt to identify this phase, several methods of analysis were used. X-ray diffraction experiments performed on extraction residues were unsuccessful because of the exceedingly small amount of residue available after etching.

Extraction replicas were analyzed by electron microscopy. Constituents associated with hot-cracks included M_6C carbides and trace amounts of chi-phase, R-phase, and MnS. Figure 6 is a micrograph of an extraction replica from a fusion zone hot-crack in a high silicon alloy. The precipitates outlining the edges of the crack were determined by selected-area electron diffraction to be M_6C carbide. Figure 7 is a selected area diffraction pattern from the phase identified by an arrow in Fig. 6. Shown is the [001] zone. The pattern, and others taken in conjunction, indicate a cubic crystal structure with a lattice parameter of approximately 10.8 Å. Inspection of Fig. 7 reveals the absence of the (200) reflection, unambiguously identifying a diamond cubic (M_6C) crystal structure (Ref. 7).

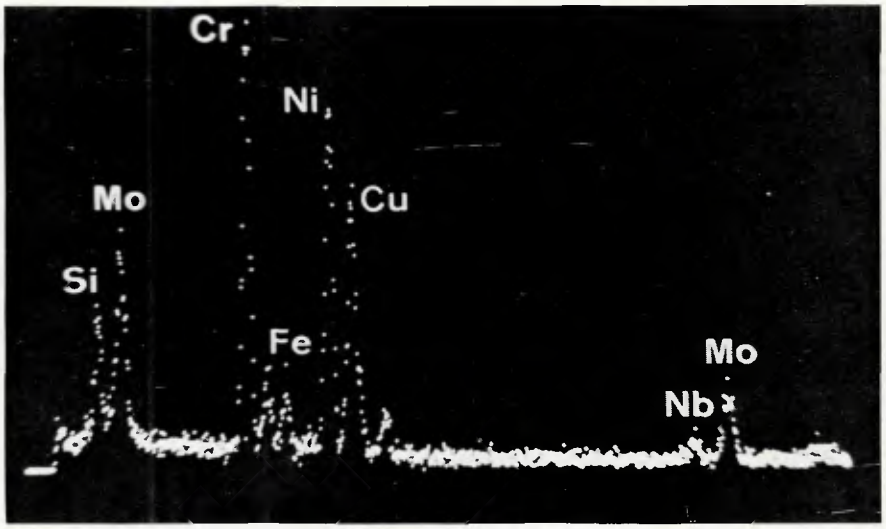

Fig. 8—STEM/EDS spectrum of M_6C carbide shown in Fig. 6

Figure 8 is a STEM/EDS spectrum of the M_6C carbide shown in Fig. 6. The chemistry is characteristic of M_6C carbide (Refs. 8,9,10). It contains large amounts of molybdenum and silicon, a high ratio of molybdenum to chromium, low iron content, and substantial nickel. M_6C has been reported to form as a eutectic constituent in nickel-base alloys having a high molybdenum content (Ref. 11). It has also been reported (Refs. 8,9,10) that M_6C carbide can dissolve from 3 to 9 wt-% silicon in stainless steels and nickel-base alloys.

Heat 31 is a CN-7M-type alloy containing 0.13% carbon. In the as-cast condition, it contained large amounts of an interdendritic eutectic constituent. Figure 9 shows an example of this constituent. Examination of TEM thin foils made from this casting revealed the lamellar constituent to be M_6C carbide. The larger, blocky phase was found to be $M_{23}C_6$ carbide.

The STEM/EDS spectra from these two phases are shown in Fig. 10. As shown in Fig. 10A, M_6C carbide again is characterized by a large molybdenum and silicon content, a high ratio of molybdenum to chromium, and substantial nickel. The $M_{23}C_6$ carbide in Fig. 10B is predominantly chromium carbide, with a low molybdenum to chromium ratio, and very little nickel. It seems likely that the $M_{23}C_6$ formed from decomposing M_6C in this alloy in a manner analogous to the same reaction in René 41 and M-252 (Ref. 12).

The thin solidification grain boundary constituent found associated with hot-cracks in high silicon alloys was analyzed using a microprobe. Figure 11 is representative of the areas analyzed. Table 5 gives the chemical analysis of the areas identified in Fig. 11.

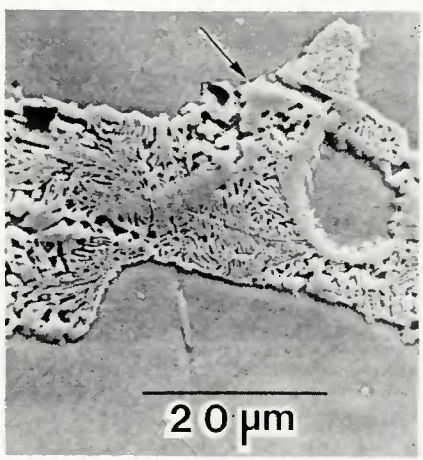

Fig. 9—SEM photomicrograph of the interdendritic eutectic constituent found in the as-cast microstructure of Heat 31. The lamellar regions are eutectic M_6C/austenite. The blocky structure (arrow) is $M_{23}C_6$

The round phase in Fig. 11 is clearly a sulfide, and predominantly a manganese sulfide, although there is some substitution of copper as the metal species. The lighter shaded phase has a composition characteristic of M_6C carbide. The apparent low carbon content is probably due to matrix effects. A high beam current, and hence a large spot size, was necessary to determine the carbon content of this phase.

Quench Experiments

Figure 12 is a metallographic section of a series of dendrite tips which were growing into the trailing edge of a weld at the instant of water quenching. A microprobe profile was taken, after repolishing, across the center dendrite shown in Fig. 12. Figure 13 shows this profile,

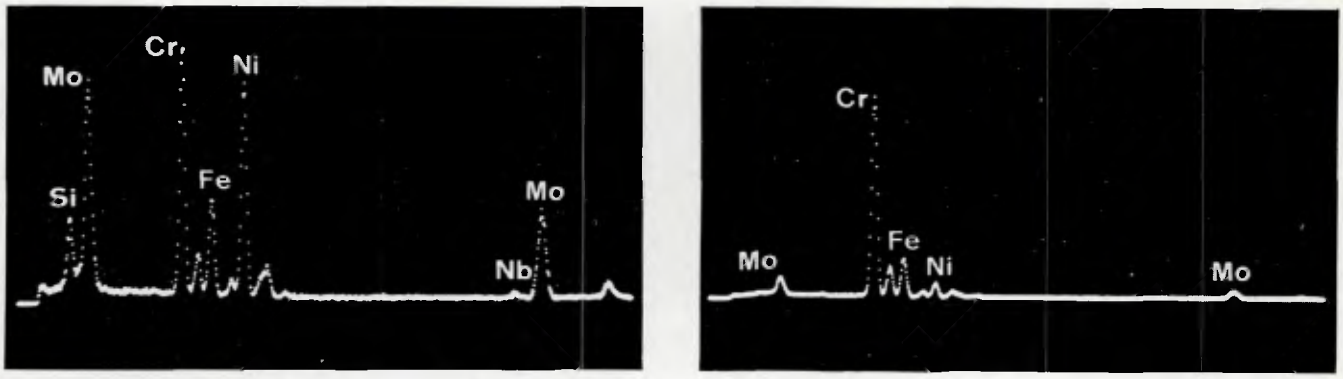

Fig. 10—STEM/EDS spectra of carbide phases found in Heat 31: A—M_6C carbide. B—$M_{23}C_6$ carbide

which reveals that all alloying elements segregate to interdendritic volumes. In particular, note that sulfur and phosphorus are found in interdendritic regions at levels several times their bulk concentration.

Discussion

The DTA results indicate that alloy CN-7M does not have an especially wide solidification temperature range relative to other stainless steels, including those which are considered readily weldable such as Type 308 stainless steel. There is no reason to believe, therefore, that the wide solidification temperature range mechanism is particularly responsible for the hot-cracking tendency of alloy CN-7M.

The analysis of Varestraint data indicates that sulfur, phosphorus, and silicon are responsible for the hot-cracking tendency of alloy CN-7M.

Both TEM and microprobe analyses revealed the presence of sulfides along hot-cracks and elemental sulfur (Fig. 13) was found to strongly segregate to interdendritic volumes. Arata *et al.* (Ref. 13) have shown that sulfide eutectics cause hot-cracking in austenitic stainless steels. Discrete phosphides were not found during this investigation. Brooks *et al.* (Ref. 14) found phosphides in austenitic stainless steels only when the phosphorus content was greater than 0.2%. Arata *et al.* (Ref. 13) had a similar experience with phosphides in Type 310 stainless steel.

Borland (Ref. 15) has suggested that the harmful effects of residual elements on hot-cracking tendencies could be related to the decrease in surface tension of the intergranular fluids caused by the segregation of these elements to final solidification volumes. It has been reported that both sulfur (Refs. 16,17) and phosphorus (Refs. 18,19) lower the surface tension of iron and steel melts, and both have been shown in this study to segregate extensively to interdendritic volumes.

The detrimental effect of silicon can be directly related to the formation of a thin film M_6C carbide/austenite eutectic at solidification grain boundaries. Two pieces of evidence support this. The first is the metallographic observation that this constituent forms only in the high silicon alloys and that more does not form in the presence of higher carbon content (up to 0.07% carbon). This implies that silicon, not carbon, is the element controlling the formation of the M_6C. The second is the observation of Gehlback and Cook (Ref. 10) during the study of carbide formation in Hastelloy N; they noted that M_6C carbide would not form in the absence of silicon, even when 16% molybdenum and 0.06% carbon was present.

The Varestraint data of Cadden (Ref. 20) also reveals the detrimental influence of silicon on CN-7M cracking properties. Brown and Koch (Ref. 21) reported that silicon increased the hot-cracking tendency of alloy 20Cb-3, a niobium-bearing wrought counterpart to CN-7M. In neither case was a cracking mechanism described.

The effect of carbon on cracking properties was slight. Fink (Ref. 22) reported that increasing the carbon content of alloy CN-7M from 0.03% to 0.05% would improve weldability. However, he gave no explanation and suggested no mechanism for the improvement. The carbon-silicon interaction was such that higher carbon contents moderated the detrimental influence of silicon. Polgary (Ref. 23) observed the same interaction in stainless steels and attributed it to a reduction in grain boundary silicate formation during solidification. It is unlikely that this mechanism is operative in the present case. No definitive explanation of this or the other interactions could be discerned. From a practical standpoint, the interactive effects have only a limited

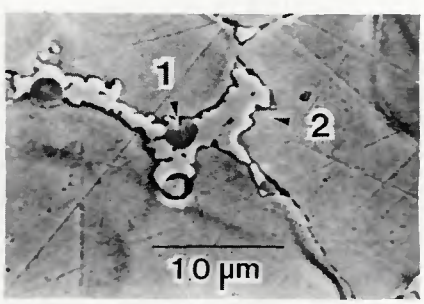

Fig. 11—Representative area undergoing microprobe analysis, Heat 5. (1) is a sulfide, (2) is eutectic M_6C carbide

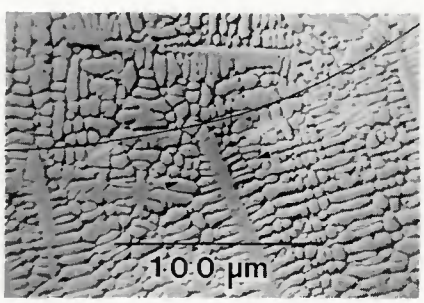

Fig. 12—Dendrite tips at quench interface (curved line). Arrows denote positions of microprobe profiles

Table 5—Microprobe Analysis Data, Wt-%

Area	Fe	Cr	Ni	Mn	Mo	Cu	Si	P	S	C
Matrix	39.90	23.72	28.76	1.68	2.05	2.78	0.76	0.00	0.06	–
1	2.46	7.90	2.34	40.20	0.90	15.26	0.47	0.03	26.13	–
2	21.97	26.27	24.31	2.30	17.44	1.82	3.28	0.44	0.21	1.50

importance, for their magnitudes are considerably less than the single element effects.

The insignificance of the effect of most of the major alloying elements on cracking susceptibility was not expected. The effect of manganese, for example, could have been diminished because it was tested only when sulfur was held relatively low. Substantial molybdenum was present in all alloys and was apparently there at high enough levels at all times to allow the formation of M_6C if silicon was also present in a critical amount. The microprobe data indicated that all alloying elements segregated to interdendritic regions during solidification, but the hot-cracking analysis revealed that only a few elements affected cracking properties. This suggests that, in general, caution be used in stating that a particular element is harmful simply because it is found as a segregate in areas associated with hot-cracking.

Conclusion

The causes of hot-cracking in alloy CN-7M are both generic to austenitic stainless steels and alloy specific. This alloy is susceptible to residual element (sulfur, phosphorus) induced hot-cracking in a manner analogous to that found in other wholly-austenitic stainless steels. Also, the addition of high levels of silicon (1%) to this alloy causes the formation of a thin film M_6C carbide/austenite eutectic which diminishes the hot-cracking resistance.

The results of this study suggest that melting and/or refining techniques can have a significant effect on hot-cracking properties. The use of virgin materials for the furnace charge and the application of a process which simultaneously melts and refines, such as the argon-oxygen decarburization (AOD) process, would be beneficial.

Acknowledgments

The authors would like to thank the Steel Founders Society of America for the financial and materials support required to complete this study. The assistance of A. M. Ritter, N. Lewis, S. David, J. Lippold, and D. Sheldon is greatly appreciated.

Portions of this work were performed at Sandia National Laboratories and supported by the U.S. Department of Energy under contract number DE-AC04-76DP00789.

References

1. Savage, W. F., and Lundin, C. D. 1965. The Varestraint test. *Welding Journal* 44(11):433-s to 442-s.

2. Savage, W. F., and Lundin, C. D. 1966. Application of the Varestraint technique to the

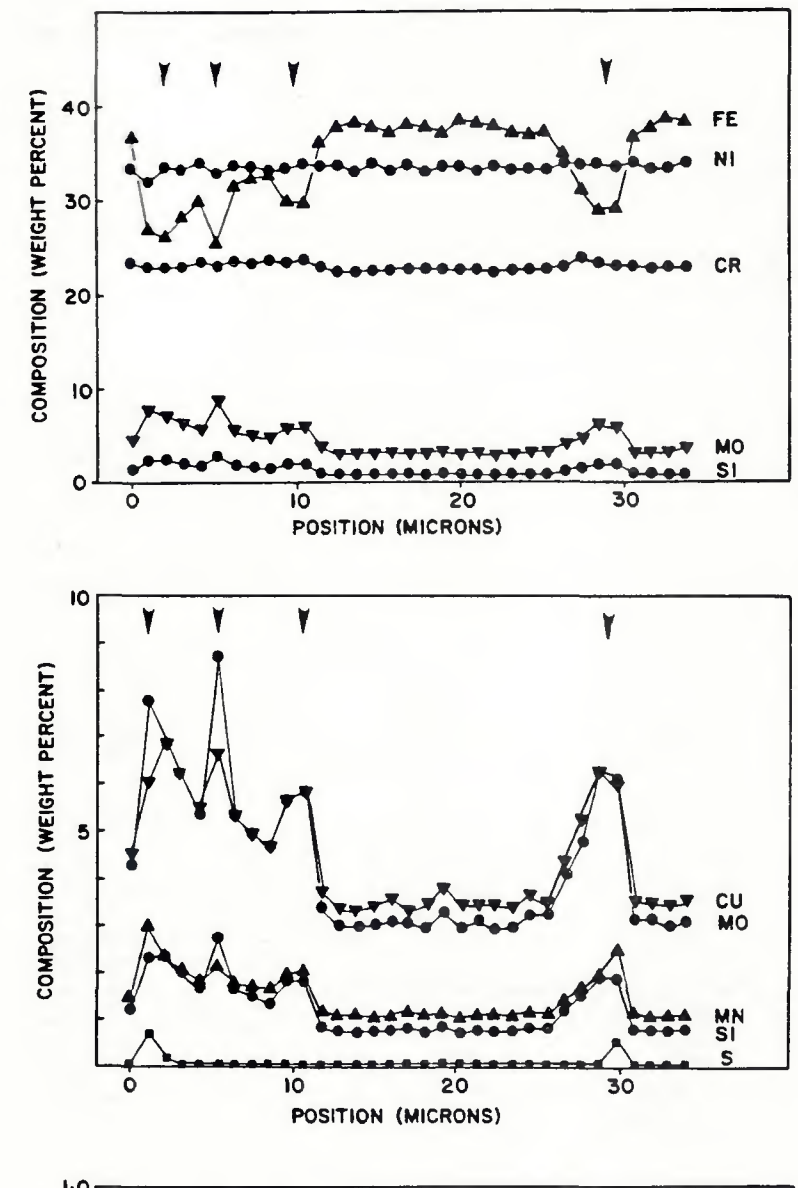

Fig. 13 – Transverse microprobe profiles along path indicated in Fig. 12. Arrows denote interdendritic regions

study of weldability. *Welding Journal* 45(11):497-s to 503-s.

3. Arata, Y., Matsuda, F., and Katayama, S. 1976 (Dec.). *Transactions of JWRI* 5(2):35.

4. Box, G. E. P., Hunter, W. G., and Hunter, J. S. 1978. *Statistics for experimenters,* p. 410. John Wiley and Sons, Inc.

5. Davies, O. L. 1979. *The design and analysis of industrial experiments,* 2nd ed., pp. 430, 486. Longman Group Ltd.

6. Yates, F. *The design and analysis of factorial experiments, bulletin 35,* Imperial Bureau of Soil Science, Harpenden, Hertz, England, Hafner.

7. Raghavan, M., Mueller, R. R., Klein, C. F., and Vaughn, G. A. 1983. *Scripta Met.* 17:1189.

8. Piearcey, B. J., and Smashey, R. W. 1967. *Trans. AIME* 239: 451.

9. Maziasz, P. J. 1979. *Scripta Met.* 13: 621.

10. Gehlbach, R. E., and Cook, S. W. 1970. *Molten-salt reactor program semi-annual report for period ending February 28, 1970.* ORNL report no. 4548.

11. Sims, C. T., and Hagel, W. C. 1972. *The Superalloys,* p. 120. Wiley-Interscience.

12. *Ibid.,* p. 56.

13. Arata, Y., Matsuda, F., and Katayama, S. 1977 (June). *Transactions of JWRI* 6(1):105.

14. Brooks, J. A., Thompson, A. W., and Williams, J. C. 1983. Variations in weld ferrite content due to P and S. *Welding Journal* 62(8):220-s to 226-s.

15. Borland, J. C. 1960. *British Welding Journal* 7:558.

16. Van Vlack, L. H. 1951. *Journal of Metals* 3:215.

17. Halden, F. A., and Kingery, W. D. 1955. *Journal of Physical Chemistry* 59:557.

18. Kozakevitch, P., Chatel, S., Urgain, G., and Saye, M. 1955. *Rev. Met.* 52:139.

19. vor dem Esche, W., and Peter, O. 1956. *Arch. Eisenhuttenw.* 27(6):355.

20. Cadden, C. H. 1981 (May). *M. S. thesis: weldability of high alloy castings.* Troy, New York: Rensselaer Polytechnic Institute.

21. Brown, R. S., and Koch, J. B. 1978. Development of a solidification crack resistant weld filler metal for a stabilized full austenitic alloy. *Welding Journal* 57(2):38-s to 42-s.

22. Fink, L. 1960. *Transactions of the American Foundryman's Society* 68:505.

23. Polygary, S. 1969 (Feb.). *Metal Construction and British Welding Journal,* p. 93.

24. Cieslak, M. J., Savage, W. F., David, S. A. 1979. Unpublished joint investigation at RPI and ORNL.

25. David, S. A., Goodwin, G. M., and Vitek, J. 1979. Solidification behavior of austenitic stainless steel filler metals. *Welding Journal* 58(11):330-s to 336-s.

26. David, S. A., and Goodwin, G. M. 1979. *Weldments: physical metallurgy and failure phenomena,* p. 19. General Electric Co.

27. Leffler, B., and Malm, S. 1977 (Feb.). *Metals Technology,* p. 81.

28. *A Guide to the Solidification of Steel.* 1977. Jernkontoret, Stockholm, p. 81.

29. Callmer, B., and Grinder, O. 1980. *Scandinavian Journal of Metallurgy,* p. 151.

Call for Papers—
Control of Casting and Welding

The Engineering Foundation Conference, Modeling and Control of Casting and Welding Processes, is scheduled for January 12-17, 1986, in Santa Barbara, Calif. The program will focus upon methods and applications of modeling and control to casting and welding processes. Both scientific fundamentals and practical applications will be emphasized.

Contributions from academic, industrial and government laboratories are solicited for the conference. Fundamental topics to be addressed include: evolution of microstructure; structure, stability and heat transfer at interfaces; modeling of heat transfer during welding; methods of process control and automation; surface tension and electromagnetic-force driven flow during welding, crystal growth and casting.

Submitted abstracts must be received by July 1, 1985. Send to Professor Sindo Kou, Dept. of Metallurgical and Mineral Engineering, 1509 University Ave., University of Wisconsin, Madison, WI 53706; or Dr. Robert Mehrabian, Dean of the College of Engineering, 1012 Engineering Bldg., University of California, Santa Barbara, CA 93106.

Call for Papers—
International Welding Research

Papers are solicited for the ASM-sponsored International Conference on "International Trends in Welding Research," to be held in Gatlinburg, Tenn., May 18-22, 1986. This eight-session symposium will cover heat and fluid flow problems in welds, solidification, solid state transformations, mechanical behavior of welds, and welding processes and process control. Conference proceedings will be published. Submit abstracts up to 300 words by November 15, 1985, to S. A. David, Materials Joining Laboratory, Metals and Ceramics Divisions, Oak Ridge National Laboratory, P. O. Box X, Oak Ridge, TN 37831. Inquiries for future information should be addressed to American Society for Metals (ASM) Conference Dept., Metals Park, OH 44073.